

Pruning vineyards: updating barcodes and representative cycles by removing simplices

Barbara Giunti*

Jānis Lazovskis†

Abstract

The barcode of a filtration and its representative cycles encode rich information often useful in data analysis. However, obtaining them can be computationally expensive. Therefore, it is useful to have methods that update them if the associated filtration undergoes small changes. There are already efficient algorithms updating a barcode if simplices exchange entrance order or are added, but not if simplices are removed. We provide an implementation to update a reduced boundary matrix when simplices in the filtration are removed. Our algorithm, the Simplicial Removal Update Procedure (SiRUP), intrinsically updates also the representative cycles, and is compatible with the twist optimizations. We show that the complexity of our algorithm is lower than recomputing the barcode from scratch and that the number of executed matrix column additions is minimal, with both theoretical and experimental methods.

MSC 2020: 55N31, 15-04, Secondary: 68Q25

Keywords: persistent homology, matrix reduction, barcode update, filtration, vineyards, simplex removal, representative cycles update.

1 Introduction

Persistent homology (PH) is a tremendously successful tool in topological data analysis (TDA), with hundreds of practical applications [GLR22]. Arguably, one of the reasons for its success is the computability of its main invariant, the **barcode** [Ott+17; Bau21; Bau+17], which represents the topology of a dataset as a collection of life spans of topological features, or **bars**. The **representative cycles** are collections of simplices (and thus, of data points) that generate the topological features encoded in the barcode, and have been demonstrably useful in practice [AP23; Li+21]. For practical purposes, the worst-case complexity of the barcode computation is cubic in the number of simplices, which becomes problematic for very large datasets. It is therefore useful to have methods to update an already computed barcode if the dataset changes a little, instead of recomputing it from scratch.

The barcode computation requires simplices to be ordered, or **filtered**, and in any ordering there are fundamentally three changes that may happen: simplices are added, simplices exchange order, or simplices are removed. In the literature, insertion and order swap of simplices has already been studied [CEM06; LN24], but no explicit, systematic work has been done on updating the barcode and the representative cycles by removal of simplices. The removal of simplices from a complex may be encoded by a zigzag filtration [DH22b; DH24], but that is not the most efficient method to remove simplices (see Example 4.2). The approaches in [CEM06; LN24] allow for removal only by swapping the simplices to the end of the filtration and then dropping them, which incurs more operations than are strictly necessary (see Section 4.4 for an extended discussion). In this paper, we fill this gap by providing an efficient method to update a barcode and the representative cycles that generate it by removing simplices.

*bgiunti@albany.edu SUNY - University at Albany, NY, USA, & Graz University of Technology, Austria

†janis.lazovskis@lu.lv University of Latvia, Riga, Latvia, & University of Aberdeen, Scotland, United Kingdom

We provide an algorithm that takes as input the boundary matrix D factored as $D = RU$, where U is the **operations matrix**, and a list L of simplices to be removed. This factorization is the usual output of barcode algorithms, as the barcode can be read directly from R . Our algorithm returns R' and U' , where $D' = R'U'$ is the matrix of the original filtration without the simplices in L . We show that our method of computing R' and U' from R and U has better theoretical complexity than factoring D' into its two factors. Moreover, we provide an implementation and experiments showing that also in practice we can expect our method to be faster.

1.1 Motivation and applications

Neuroscience. Computational neuroscience has recently been harnessed with topological tools [Rei+17; Con+22; Col+22], which allow for a dramatic simplification. A common approach is to consider neurons as data points and synapses as (directed) connections between the data points; or a cell body and branchings as data points and the cell material in between as connections. This describes a directed graph, whose *clique complex* is a collection of simplices with a natural filtration by dimension and ordering. Neuron activity (either firing or not firing) gives a sequence of filtrations over time, defined by the active subcomplex. When a collection of neurons fires in one time interval and does not fire in the next, the change is reflected as simplices removed from the filtration. Datasets in neuroscience often have several thousands of neurons, with current experiments often carried out on smaller subsets because the computational complexity is too high. Therefore, it is useful to have the possibility to “pay the price” by computing once the whole the barcode of datasets, and then perform only small and local update when different neurons fire.

Manifold learning. As a machine learning method, manifold learning reduces the dimensionality of the data while preserving important features. Non-linear dimensionality reduction is often performed by *auto-encoders*, which can be paired with PH to preserve more information, in particular topological information [Moo+20]. The simplest auto-encoders attempt to reduce the dimension of the manifold globally, without respect to local features. Using multi-charts auto-encoders is a way to keep local information, taking care to appropriately relate the barcodes of each chart. However, there is some fine-tuning to be done to choose the right number and type of charts, balancing efficiency and information. Every time charts are modified, the barcode needs to be recomputed. With our method, it is enough to make an initial computation which can be continuously updated whenever charts are modified.

Streaming, dynamic, and noisy data. In settings where data is incomplete, or regularly being updated, any sort of topological signature on the data will have to be updated as frequently as the underlying data is updated [PH15]. This area has only recently been developing [Ede+04; KMS20], but its general setting of continuously responding to new inputs makes it a fertile area for many directions, emphasized by the proliferation of data and data channels in the 21st century. This can also be applied to situations where the full topological analysis of a dataset is not possible because the total size is too big. In this case, one can begin to analyze a subset of the input, and then add and remove data to look for meaningful topological information without exceeding the computational capability.

1.2 Related work

Changes in PH over a time parameter have been widely studied [CEF13; Ede+04; Oes+17; Hic23], with algorithmic advances for dynamic computations laid in [CEM06; KMS20], introducing methods to update the reduced boundary matrix when the order of simplices changes. Building on this work, the authors of [LN24] provide efficient methods to update the barcode of any filtration, if simplices are inserted, their ordered changed, or if the simplices at the end of the filtration are removed. This is the only case we are aware of a work explicitly discussing the updating of barcode following the removal of simplices, though it uses the order changing method of [CEM06] to push the simplices to

the end of the filtration and then drops them. In Section 4.4.2 we detail the differences in procedure and efficiency with our method.

In [LN24], removal is reduced to swapping: keeping R upper triangular while moving the simplex to be removed to the end of the filtration implies that simply dropping the last column maintains the correct pivot pairing of the modified filtration, as the last column can not be added to any other columns. While, as shown in [LN24], it is possible to implement a removal working around the standard barcode algorithm (Algorithm 1), this is not very efficient, as many operations are canceling each other. Our method skips several of these redundant operations by considering the removal in its own right.

Recent work by Dey–Hou [DH22b; DH24] computes the barcode of a *zigzag* filtration, generalizing from a linear filtration order. Their method may be adapted to update the barcode by removal of simplices, by inserting at the end of the filtration backward maps, each map removing a simplex. Their *forward switch* and *inward contraction* moves (see [DH22b; DH24]) allow their methods to be used across a wide range of filtrations. However, their approach doubles the length of the filtration as it is concerned with a wide class of changes. While both their and our methods require in the worst case an amount of column additions that is linear in the number of simplices, we demonstrate ours always performs less or at most the same number of column additions, and has a more direct computation (see Section 4.4.1).

2 Background

Throughout the paper, we restrict to \mathbb{Z}_2 coefficients (so all additions are modulo 2) and finite simplicial complexes.

Matrix reduction. Given a matrix D , we denote by $D[i]$ its i -th column, and by $D[i, j]$ the i th element of its j th column. As in linear algebra, the **pivot** of $D[i]$, here denoted by $\text{piv}(D[i])$, is the row index of the lowest non-zero element in column i . A matrix is **reduced** if all its non-zero columns have unique pivots. The standard PH **reduction** algorithm for making an unreduced matrix reduced is recalled in Algorithm 1, here referred to as SBA - the Standard Barcode Algorithm [ELZ00].

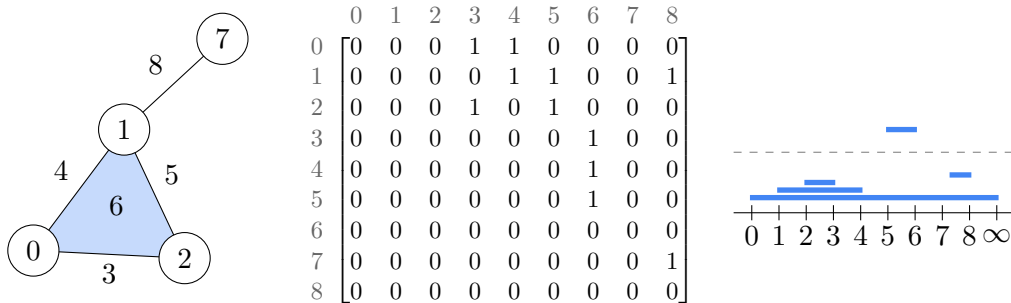


Figure 1: A simplicial complex K (left) with its simplices indexed, its (unreduced) boundary matrix (middle) corresponding to the simplex-wise filtrations, and its barcode (right), with dimension 0 bars below the dashed line and dimension 1 bars above the dashed line.

Simplicial complexes and filtrations. Given a finite set V , an k -simplex (over V) is a subset of V of size $k + 1$. Whenever there is a relationship $\tau \subsetneq \sigma$ among simplices, the simplex τ is called a **face** of σ and σ is called a **coface** of τ . If, in addition, $\dim(\tau) = \dim(\sigma) - 1$, then τ is also called a **facet** of σ , and σ is called a **cofacet** of τ . A **simplicial complex** is a set K of simplices that is closed under non-empty subsets, that is, if $\tau \subset \sigma$ and $\sigma \in K$, then $\tau \in K$. The **star** of a

simplex $\sigma \in K$ is the collection of simplices containing σ , written $\text{st}(\sigma) := \{\tau \in K : \sigma \subseteq \tau\}$. Note that $\text{st}(\sigma)$ is in general not a simplicial complex, but $K \setminus \text{st}(\sigma)$ is a simplicial complex for all $\sigma \in K$.

A **filtration** of a simplicial complex K is a sequence $\mathcal{F} := K_1 \subseteq \dots \subseteq K_n$ of simplicial complexes, with $K_n = K$. Given an ordering \preccurlyeq of all the simplices in a simplicial complex $K = \{\sigma_1, \dots, \sigma_n\}$ that respects the face relation (that is, if $\sigma_i \subseteq \sigma_j$ then $\sigma_i \preccurlyeq \sigma_j$), the **simplex-wise filtration** of K is defined by $K_i = \{\sigma_1, \dots, \sigma_i\}$. This is the default filtration for our purposes. The variable n denotes the number of simplices in the simplicial complex, and thus the number of steps in the filtration. The **entrance time** of simplex σ_i , or step in the filtration when σ_i first appears, is i . A filtration \mathcal{F} has a naturally associated $n \times n$ **boundary matrix** D , whose (i, j) -entry $D[i, j]$ is 1 if the i th simplex is a facet of the j th simplex, and 0 otherwise, with simplices ordered by their entrance times. With a little abuse of notation, we use the indices from 1 to n also to denote the columns in D .

Homology. We provide an intuition of homology and its computation, following the setup of singular homology, and refer the reader to [EH10; Oud15; DW22] for formal details.

Given a simplicial complex K , we can consider sums of simplices of the same dimension, computed as sums of the respective columns in the boundary matrix. For example, the sum $e_2 + e_3$ of the simplicial complex in Figure 2, indicated by dashed lines, is recorded in the boundary matrix by adding the second column to the third columns. As a result, the **boundary** of the sum $e_2 + e_3$ is $v_1 + v_2$, as in Figure 2(b), indicating that the boundary contains v_1 and v_2 , which is exactly what we expect from the picture. If we add also e_1 , we obtain a closed path, which, intuitively, has no boundary and whose boundary column is indeed zero, as in Figure 2(c). A formal sum whose boundary column is zero is called a **cycle**, which also reflects the intuition of a closed loop.

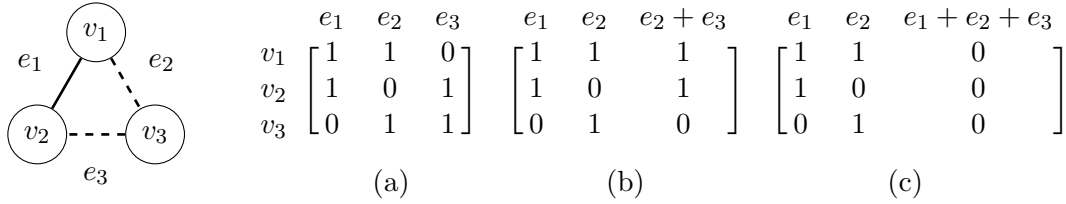


Figure 2: A simplicial complex (left), the sub-matrix of its boundary matrix given by the edges and their boundaries (a), the formal sums $e_2 + e_3$ (dashed) and $e_1 + e_2 + e_3$ (dashed and solid), (b) and (c) respectively.

If the simplicial complex in Figure 2 had also the 2-simplex with edges e_1, e_2, e_3 , then the formal sum $e_1 + e_2 + e_3$ would be its boundary. Having a cycle in dimension k that is the boundary of a formal sum of simplices in dimension $k + 1$ means the cycle would not be captured by homology, as its **homological classes** are defined as “cycles modulo boundaries.” Without such a 2-simplex, the cycle does not correspond to a boundary, and so is a **representative cycle** of a homological class, that is, a 1-dimensional hole. Note that a class may have several representative cycles, whenever their difference does not exist in homology. This intuition gives us an informal definition of the main object in homology: *Nontrivial homology classes are sums of simplices that are cycles, but not boundaries.*

Persistent homology. Given a filtration over a simplicial complex, its **persistent homology** is given by the homology of each complex in the filtration, together with morphisms connecting them. When a simplex σ enters the filtration, one of three things may happen:

1. adding the column of σ to an existing sum of simplices makes the boundary of the sum zero; or
2. adding the column of σ does not make any existing sum zero, and the boundary of σ is not a cycle; or

3. the boundary of σ is the cycle of a formal sum of simplices entering earlier.

Case 1 corresponds to the first occurrence in a filtration of a nontrivial homology class c at the entrance time of σ . This time is called the **birth time** of c class, and σ is called a **positive** simplex that is **born** at this entrance time and which **creates** the class c . In case 2, there is no change in homology classes. Case 3 corresponds to a filtration step without a homology class c that existed at the previous step. This time is called the **death time** of c , and σ is called a **negative** simplex that is **killed** at this time and which **kills** the class c . The interval between the birth and death times is called a **bar**, and the collection of bars is represented in a **barcode**, as in Figure 1 (right). In persistent homology, cycles that are not boundaries at some step (but may be boundaries later) are still called representative cycles.

The barcode of a filtration \mathcal{F} is computed from its boundary matrix D , usually using (variations of) SBA [ELZ00]. The key part of any barcode computation is finding the *pivot pairs*. Let $D[\geq l, \leq f]$ denote the submatrix of D given by the last l rows of the first f columns of D . As shown in [ELZ00], (i, j) is a **pivot pair** if and only if

$$\begin{aligned} \text{rank}(D[\geq i, \leq j]) - \text{rank}(D[\geq i+1, \leq j]) \\ + \text{rank}(D[\geq i+1, \leq j-1]) - \text{rank}(D[\geq i, \leq j-1]) = 1 \end{aligned} \quad (1)$$

Given a pivot pair (i, j) in a simplex-wise filtration, the simplex σ_i creates a homological class and σ_j kills that class, and we draw the interval from i to j as a bar in the barcode. Most computations of the barcode [ATV14; Bau21; Bau+17; The15; HG16; Mor10; Pér+21] implement, with various speed-ups, SBA, which we report here for self-containment with the slight modification of keeping explicit track (in Line 6) of the performed column operations in the matrix U .

Algorithm 1: SBA - STANDARD BARCODE ALGORITHM [ELZ00]

Input: Boundary matrix D , identity matrix I
Output: Reduced matrix R , operations matrix U

```

1  $R \leftarrow D$ 
2  $U \leftarrow I$ 
3 for  $j = 1, \dots, n$ 
4   while there exists  $j' < j$  for which  $\text{piv}(R[j']) = \text{piv}(R[j]) \neq 0$ 
5      $\text{add } R[j'] \text{ to } R[j]$ 
6      $\text{add } U[j'] \text{ to } U[j]$ 
7 return  $R, U$ 
```

The pivots of the resulting matrix R are precisely the pivot pairs of the simplex-wise filtration given by D , hence the barcode can be read directly off R . Note that SBA keeps track of the column operations used to reduce the matrix by storing them in U , giving the factorization $R = DU$. The matrix U is useful in general to get representative cycles, as they describe not only the existence, but also the location of a hole in the data. Our method, presented in Sections 3 and 4.3, provides updates to both U and R when removing simplices from the filtration. At the end of SBA, U is upper triangular. However, several variants of the SBA obtain a decomposition $R = DU$ where U is not upper triangular, but R still contains the correct pivot pairs [Bau+24]. Even though other methods implementing barcode updates (such as [CEM06]) require U to be upper triangular, we do not require it, mostly to avoid unnecessary extra computation steps.

3 Removing simplices

Let \mathcal{F} be a filtration of a simplicial complex K and $\{\tau_1, \dots, \tau_t\} \subseteq K$ a set of simplices to be removed from \mathcal{F} . Let $L = \bigcup_{i=1}^t \text{st}(\tau_i)$ be the union of the stars of all the simplices τ_i . We now introduce a method to update the reduced boundary matrix of \mathcal{F} to the reduced boundary matrix of the

filtration \mathcal{F} without the simplices in L , which we denote by $\mathcal{F} \setminus L$. By definition of star, $\mathcal{F} \setminus L$ is a filtration.

Our main algorithm is SiRUP (Algorithm 2). For the purposes of this algorithm, a zero column is considered to have -1 as a pivot, that is, the pivot of a zero column is higher than the one of any other non-zero column.

Algorithm 2: SiRUP- SIMPLICIAL REMOVAL UPDATE PROCEDURE

Input: Reduced matrix R , operations matrix U , list of simplices to be removed L
Output: Updated reduced matrix P , updated operations matrix V

```

1  $P \leftarrow R$ 
2  $V \leftarrow U$ 
3 for  $\sigma_j \in L$ 
4    $A = \{i : V[j, i] \neq 0, i \neq j\} = \{A_1, A_2, \dots\}$  in increasing order
5    $B = \{A_0 = j\} \cup \{A_i \in A : \text{piv}(P[A_i]) < \text{piv}(P[A_t]) \ \forall t < i\}$  in increasing order
6   for  $i \in A$  in decreasing order
7      $k \leftarrow$  the smallest index in  $B$  such that  $\text{piv}(P[B_k]) \leq \text{piv}(P[i])$ 
8     if  $i = B_k$ 
9        $k \leftarrow k - 1$ 
10    add column  $B_k$  to column  $i$  in  $P$  and in  $V$ 
11  remove  $P[j]$ ,  $V[j]$ , and row  $j$  in  $P$  and in  $V$ 
12 return  $P, V$ 

```

The correctness of SiRUP is proved by Theorem 3.5, using the correctness of NAIVE REMOVAL (Algorithm 3). The correctness of NAIVE REMOVAL, that is, the claim that it produces same pivot pairing at the SBA on $\mathcal{F} \setminus L$, is immediate, as Line 3 in NAIVE REMOVAL undoes all column additions in which elements of L were involved, and Line 9 ensures that the output is reduced.

Algorithm 3: NAIVE REMOVAL

Input: Reduced matrix R , operations matrix U , list of simplices to be removed L
Output: Updated reduced matrix P , updated operations matrix V

```

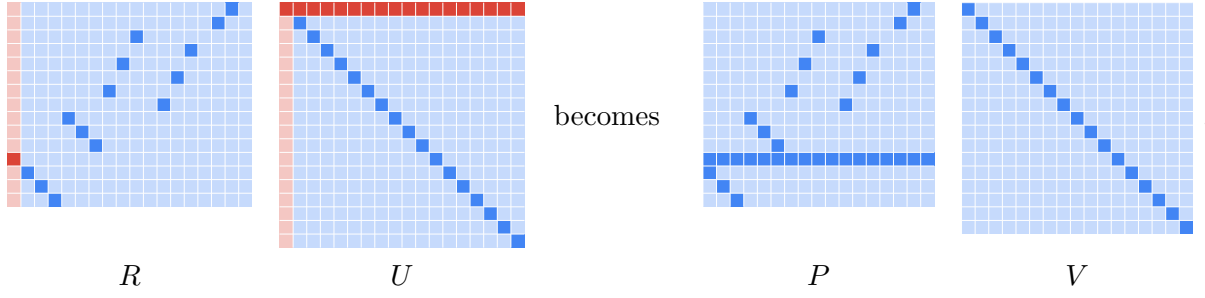
1  $P \leftarrow R$ 
2  $V \leftarrow U$ 
3 for  $\sigma_j \in L$ 
4    $A = \{i : V[j, i] \neq 0, i \neq j\}$  sorted in increasing order
5   for  $i \in A$  in increasing order
6      $V[i] \leftarrow V[i] + V[j]$ 
7      $P[i] \leftarrow P[i] + P[j]$ 
8   remove  $P[j]$ ,  $V[j]$ , and row  $j$  in  $P$  and in  $V$ 
9   call SBA( $P, V$ )
10 return  $P, V$ 

```

The key difference between the two algorithms is that SiRUP skips repeated column additions, as made precise by Lemmas 3.3 and 3.4. The addition of zero columns may also be skipped, when $P[B_k]$ is zero in Line 10, to reduce even more the number of operations. The efficiency of SiRUP is proved in Proposition 3.6, and demonstrated on practical examples in Section 5. An example to provide intuition on how SiRUP is built on top of NAIVE REMOVAL is given by Example 3.1.

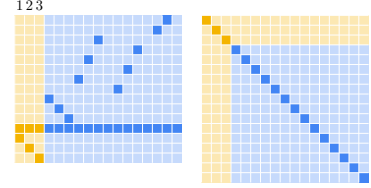
Example 3.1. Assume \mathcal{F} is a filtration and σ a simplex in it, with associated matrix reduction $R = DU$ performed by SBA, restricted to the columns in dimension $\dim(\sigma)$. Consider now the

execution of NAIVE REMOVAL with $L = \{\sigma\}$, up to and including Line 8, after which

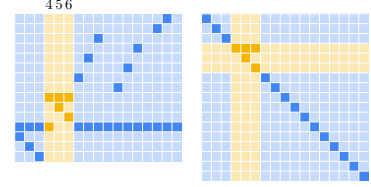


Now we consider the effect of executing SBA in Line 9, moving left to right through P .

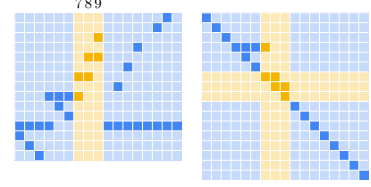
Columns 1,2,3: The first three columns in P are unaffected, as their pivots are unique. Their pivots are unchanged by NAIVE REMOVAL.



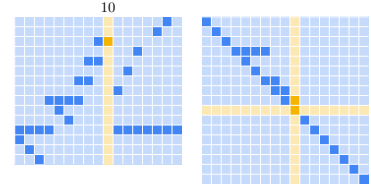
Columns 4,5,6: Column 4 is unaffected by SBA, retaining the pivot of the removed column, and then is added to columns 5 and 6, which then have unique pivots. Comparing to the input matrix R , column 4 has gotten a new pivot, while columns 5 and 6 have retained their original ones.



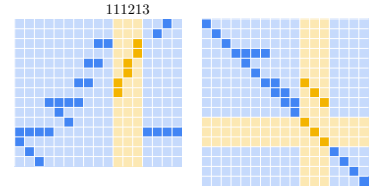
Columns 7,8,9: Column 4 is now added to column 7, whose pivot is then unique. Columns 4 and 7 are added to column 8, and columns 4, 7, and 8 are added to column 9, both with a similar result as column 7. All of these columns have gotten a new pivot compared to R .



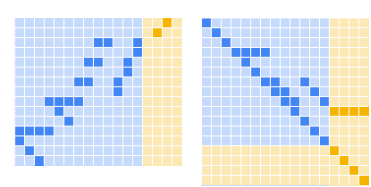
Column 10: Column 10 was a zero column in R , but now has the pivot of the removed simplex σ as its only non-zero element. Columns 4, 7, 8, and 9 are added to it, at each step bringing the pivot higher. This column has gotten a new pivot compared to R .



Columns 11,12,13: Column 11 gets columns 4, 7 added to it, leaving it with the same pivot as in R . Column 12 gets columns 4, 7, and 8 added to it, and column 13 columns 4, 7, 8, and 9, to obtain unique pivots, which are again the same as in R .



Columns 14,15,16,17: The action of NAIVE REMOVAL on all of these columns is the same. Each column gets columns 4, 7, 8, 9, and 10 added to it, resulting in unique pivots that are the same as in R .



The key insight is that NAIVE REMOVAL executes 59 column additions, but many of them simply undid each other, as the computations are modulo 2. In the end, only 18 matrix operations are necessary: 14 column additions indicated by V , and 4 column / row removals for the simplex that was removed.

Remark 3.2. To give some more intuition about the sets A and B in SiRUP, note that in Example 3.1, the set A contained the indices of all the columns (except σ), as demonstrated by top row of U having all nonzero elements in. The set B can be thought of as being constructed while going left to right through $\{A_0 = j\} \cup A$, and adding an index to B whenever the encountered pivot is higher (smaller index) than all pivots before. We saw that

$$P_{\text{before}} = \begin{array}{|c|} \hline \text{[Matrix with blue squares and one red square at the bottom left]} \\ \hline \end{array}, \quad P_{\text{after}} = \begin{array}{|c|} \hline \text{[Matrix with blue squares and several white squares around them]} \\ \hline \end{array}, \quad (2)$$

where P_{before} is P as it was before Line 4, and P_{after} is P as it was after Line 9. The elements of B are emphasized with squares around them. Notice that the columns for which pivots change are captured precisely by B , and the new pivots are defined by the order of elements in B .

We now make the intuition from the example rigorous and prove the correctness of SiRUP, beginning with two preliminary results about NAIVE REMOVAL and the set B defined in Line 5 of SiRUP. For ease of notation, given a fixed $\sigma_j \in L$, we write $P^\triangleleft[i]$ for the state of $P[i]$ at the beginning of step j in the for-loop of Line 3 of NAIVE REMOVAL, and $P^\triangleright[i]$ for the state of $P[i]$ at the end of that step, with analogous notation for V . For convenience, the elements of B from Line 10 of SiRUP are indexed beginning with 0, that is, $B = \{B_0 = j, B_1, B_2, \dots\}$.

Lemma 3.3. *In NAIVE REMOVAL, for every $B_i \in B$ with $i > 0$, we have*

1. $\text{piv}(P^\triangleright[B_i]) = \text{piv}(P^\triangleleft[B_{i-1}])$, and
2. $V^\triangleright[B_i] = V^\triangleleft[B_i] + V^\triangleleft[B_{i-1}]$.

This lemma makes precise the cases in which NAIVE REMOVAL changes a pivot. For example, in the extreme case that $B = A$, this lemma describes how

$$\begin{array}{cc} \begin{array}{|c|} \hline \text{[Matrix R with blue squares]} \\ \hline \end{array} & \begin{array}{|c|} \hline \text{[Matrix U with red squares]} \\ \hline \end{array} \end{array} \text{ becomes } \begin{array}{cc} \begin{array}{|c|} \hline \text{[Matrix P with blue squares]} \\ \hline \end{array} & \begin{array}{|c|} \hline \text{[Matrix V with red squares]} \\ \hline \end{array} \end{array}. \quad (3)$$

Proof. This follows by strong induction on the elements in B .

For the base case $i = 1$, first note that $B_0 = j$. The column $P[B_1]$ is the left-most column with pivot higher than that of column B_0 , and so it acquires the pivot of $P[B_0]$. As P was reduced, the pivot $\text{piv}(P[B_0])$ was unique among all previous pivots, so after removing $P[B_0]$, $\text{piv}(P^\triangleright[B_1])$ is unique among all previous pivots.

For the inductive step, consider the column $P[B_i]$, to which we must add $P[j]$ in Line 7 of NAIVE REMOVAL. In Line 9, where $\text{SBA}(P, V)$ is executed, at the beginning of step B_i of the for-loop in Line 3 of SBA, the inductive hypothesis on P for $i = 1$ gives us that column $P[B_1]$ is the only column with the same pivot as the column $P[B_i]$, and so $P[B_1]$ must be added to $P[B_i]$. Now column $P[B_i]$ has the pivot $\text{piv}(P^\triangleleft[B_1])$, as the two earlier additions of $P[j]$ to each of $P[B_1]$ and $P[B_i]$ by SBA cancel each other out. Again by the inductive hypothesis on P , now for $i = 2$, $P[B_2]$ must be added to $P[B_i]$, as these two columns have the same pivot. Now $P[B_i]$ has the pivot $P^\triangleleft[B_2]$, by the inductive hypothesis on V for $i = 2$. This pattern continues until and including $P[B_{i-1}]$, as then $P[B_i]$ is the first column to have the pivot of $P^\triangleleft[B_{i-1}]$. Then step B_i of the for-loop in SBA finishes, as the pivot of $P[B_i]$ is now unique among all columns to its left.

By strong induction, the claim holds for all elements of B . \square

Note that the second statement of Lemma 3.3 implies the first statement, but we make the distinction to emphasize the effect on pivots. The second preliminary result follows a similar argument, while considering all other affected columns.

Lemma 3.4. In NAIVE REMOVAL, for every $A_i \in A \setminus B$,

1. $\text{piv}(P^\triangleright[A_i]) = \text{piv}(P^\triangleleft[A_i])$, and
2. $V^\triangleright[A_i] = V^\triangleleft[A_i] + V^\triangleleft[b]$,

where b is the first element in B such that $\text{piv}(P[b]) \geq \text{piv}(P^\triangleleft[A_i])$.

This lemma makes precise the cases in which NAIVE REMOVAL does not change a pivot. For example, in the extreme case that $B = \{j\}$, this lemma describes how



$$\begin{matrix} R & U \end{matrix} \text{ becomes } \begin{matrix} P & V \end{matrix} . \quad (4)$$

Proof. Consider some $A_i \in A \setminus B$, with $b = B_k$ as in the statement.

After $P[j]$ has been added by Line 7, SBA is executed in Line 9. We concentrate on the stage of SBA in which column A_i is being considered, i.e. after all columns to the left of column A_i have been reduced. We claim that SBA performs precisely k column additions to column A_i , with the column $V^\triangleright[A_i]$ fully described by the telescoping sum

$$V^\triangleleft[A_i] + V[B_0] + V^\triangleright[B_1] + \cdots + V^\triangleright[B_k] \equiv V^\triangleleft[A_i] + V^\triangleleft[B_k], \quad (5)$$

simplified using Lemma 3.3. This is straightforward if $k = 0$, as then the addition of $P[j] = P[B_0]$ to column A_i does not change the pivot of column A_i .

For $k \geq 1$, the claim follows by observing that the pivot of $P[A_i]$ is now $\text{piv}(P[B_0])$, and so SBA will add $P^\triangleright[B_1]$ to it. Columns $P^\triangleright[B_{k'}]$, for increasing $k' = 1, 2, \dots$, will continue to be added to $P[A_i]$, and the pivot of $P[A_i]$ will keep changing to $\text{piv}(P^\triangleright[B_{k'}])$, until its pivot is unique (or it is the zero column). This will occur after k additions, as that is the first time that the sum in Equation (5) leaves the column $P[A_i]$ with the pivot $\text{piv}(P^\triangleleft[A_i])$, as at this step $\text{piv}(P^\triangleright[B_{k+1}])$ is finally higher (smaller index) than $\text{piv}(P^\triangleleft[A_i])$. The pivot $\text{piv}(P^\triangleleft[A_i])$ is unique, as the input matrix was reduced.

Hence the claim for SBA holds, and the consideration of column A_i ends after k additions. \square

These two results allow us to prove our main statement.

Theorem 3.5. Let \mathcal{F} be a filtration of a simplicial complex K and $L = \bigcup_{i=1}^t \text{st}(\tau_i)$, where $\{\tau_1, \dots, \tau_t\} \subseteq K$ is a set of simplices to be removed from \mathcal{F} . Using a reduced matrix and operations matrix for \mathcal{F} as input, the output of SiRUP is a reduced matrix and operations matrix for $\mathcal{F} \setminus L$.

Proof. First note that the only modification of the input reduced matrix in SiRUP is done in Line 10, which is inside a for-loop iterating over all A_i in decreasing order. Fix $A_i \in A$. If $A_i \in B$, by Lemma 3.3 the modification is the same as in NAIVE REMOVAL. If $A_i \in A \setminus B$, by Lemma 3.4 the modification is the same as in NAIVE REMOVAL. Indeed, as the for-loop in Line 6 is done in reverse, the column that is added to $P[A_i]$ is $P^\triangleleft[b]$, not $P^\triangleright[b]$, as the index of b in A is necessarily smaller than the index i of A_i . This follows by the definition of b in Line 7 and the special case for elements of B in Line 8.

Hence the modifications of the reduced boundary and operations matrices by SiRUP precisely match those of NAIVE REMOVAL, and the statement holds. \square

Note that the above arguments can be extended to fields over a prime $p \neq 2$. Indeed, the skipping of repeated operations hinges on whether an element is zero or not, rather than in its exact value.

Proposition 3.6. Let n be the number of simplices in the filtration \mathcal{F} and m the number of simplices in L . Then SiRUP has worst case complexity $O(mn^2)$.

Proof. The for-loop in Line 3 is executed m times. Constructing the list A in Line 4 requires at most n operations, as each column of V (and P) has to be considered once. The construction of list B in Line 5 may be done at the same time, as the pivot of every column has to be compared with the highest (smallest index) pivot seen so far in the construction of A . If it is higher (smaller index), then that column index is added to B . Identifying b in Line 7 has complexity $O(|B|) = O(n)$, as at most every element in B has to be considered. Adding each column in Line 10 is an $O(n)$ operation. The removal operations in Line 11 require a constant number of operations, independent of m or n . Hence the worst case complexity is $O(mn^2)$. \square

Conversely, the complexity of computing the barcode of $\mathcal{F} \setminus L$ with SBA is $O((n - m)^3)$. In Section 5 we compare the experimental running times of SiRUP and implementations of SBA[Bau+17], demonstrating that the former is always better when recomputing from scratch and outputting the representative cycles, and almost always better if one is only interested in the barcode.

Note that the size of A is bounded above by the number of simplices in dimension $\dim(\sigma_j)$. In particular, it is usually the case that $|A| \ll n$, that is, each column is added only to a small number of other columns. We also note that if $|A| = 0$, then σ_j must be a maximal simplex (that is, a simplex without cofaces).

Minimality. In addition to being a valid algorithm that updates the boundary and operations matrices, SiRUP provably executes the least amount of column additions necessary to keep the representative cycles of a filtration updated after a simplex σ has been removed. This follows as exactly one column addition is done for every cycle in which σ appears, or equivalently, for every column in the operations matrix in which the row of σ is nonzero.

It may be true that some of these column additions may not change the barcode (as is the case for columns 1,2,3,5,6 and 11 through 17 in Example 3.1), but without the column additions, the cycle representatives can not be correctly identified from the operations matrix. Even more, not performing these column additions may lead to incorrect identification of affected simplices if the process is repeated on the output.

Relation to twist. A standard optimization of SBA called **twist** [CK11; BKR14] puts many columns to zero without doing the column additions that would reduce them. This optimization, using the fact that the boundary of a boundary is zero, is commonly used in barcode algorithms, as it speeds up the computations considerably, especially when combined with cohomology [CK11; Bau+17; Bau21] or by doing row additions [Giu21]. An example of the effect is described in Figure 3.

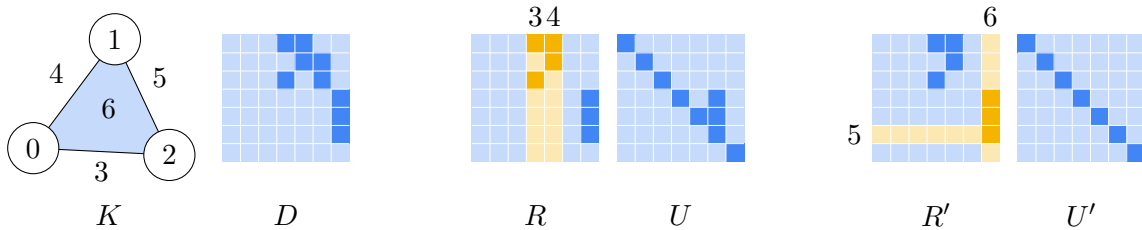


Figure 3: A simplicial complex K and its unreduced boundary matrix D (left), factored as $R = DU$ by SBA, and the outputs with clearing (right) and without (center). Clearing puts column $i = 5$ of the boundary matrix R' to zero if and only if there is a pivot pairing $(i, j) = (5, 6)$. That is, if the formal sum corresponding to column $j = 6$ kills the homological class generated by simplex corresponding to row $i = 5$.

This optimization is compatible with our method and may be selected in our implementation of SiRUP [GL24] with the flag `--twist`. Note that the operations matrix does not encode the operations made to zero out column i when clearing is used. To retrieve this information, we take as a representative cycle of column i the simplices in the boundary of column j . This same approach

may be used to update the reduced boundary matrix when swapping the order of simplices [CEM06], as the matrix U in the factorization $R = DU$ is essential for such an update.

4 Understanding removal

We now analyze different aspects of removing simplices at the geometric and barcode level, and discuss the necessity and implications of updating U .

4.1 Geometric interpretation

Given a filtration motivated by geometry, such as the Vietoris–Rips filtration, it may seem that swapping the columns in Line 4 of SiRUP is disrupting local information of the simplicial complex. We do need to be careful in keeping track of the entrance times, since the geometric length at which a removed simplex enters cannot be recomputed with only information from the other simplices. Fortunately, geometrical information encoded as algebraic information is not lost, as demonstrated by Figure 4.

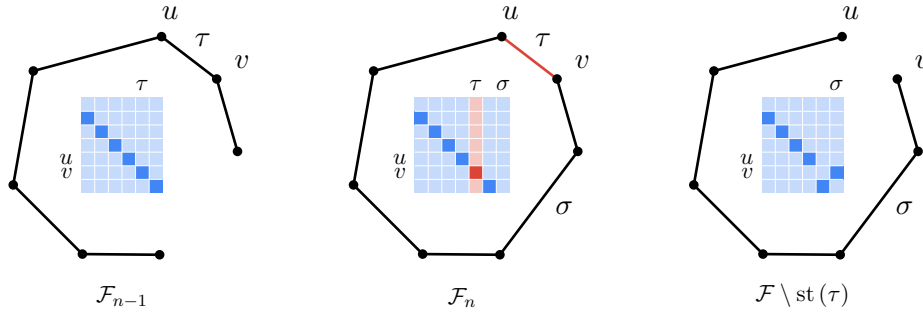


Figure 4: The penultimate step (left, \mathcal{F}_{n-1}) and final step (middle, \mathcal{F}_n) of a filtration of a simplicial complex, and the filtration after removing a simplex (right, $\mathcal{F} \setminus \text{st}(\tau)$). The reduced boundary matrix corresponding to each step is also given.

In this example, the last step of the presented filtration (Figure 4, middle) adds the edge σ , which closes a cycle and defines a pivot pair $(\sigma, -)$ in R . Hence σ is a positive simplex, that is, the column of σ in R becomes zero by adding all the other edges in the cycle to it. The removal of the edge τ (Figure 4, right) breaks the cycle, so σ should no longer be a positive simplex. However, the formal sum formed by all edges except τ has a boundary given by the same vertices as those of τ . One of these vertices, say v , represents a connected component that was originally killed by τ . After the update that removes τ , the vertex v is killed by the formal sum stored in the column of σ . In practice, there may be more than one representative chain having the same boundary as the removed simplex, so while the new pivot need not have a unique column, such a column containing the pivot will always exist. The same description holds in higher dimensions.

4.2 Updating the barcode

When two simplices swap order in a filtration, there are well-understood changes that happen to the barcode, fully described in [CEM06]. Conversely, when a simplex and its cofaces are removed, it is not as straightforward to succinctly describe what happens to the barcode, as each of the cofaces is either creating or destroying a homological class. Note that this is also the case when we insert a simplex and its cofaces. Some examples of simplex removal and the effects on the barcode are demonstrated in Figure 5.

Note that Figure 5.(c) may be generalized from 5 to N 2-simplices as cofaces, creating $N - 1$ infinite bars in dimension 1. This construction can be realized in higher dimensions as well, creating “fans” of k -simplices whose maximal face is removed when the central facet, a shared $(k - 1)$ -simplex, is removed, triggering a change that adds $N - 1$ infinite bars in dimension $k - 1$. Note that if τ

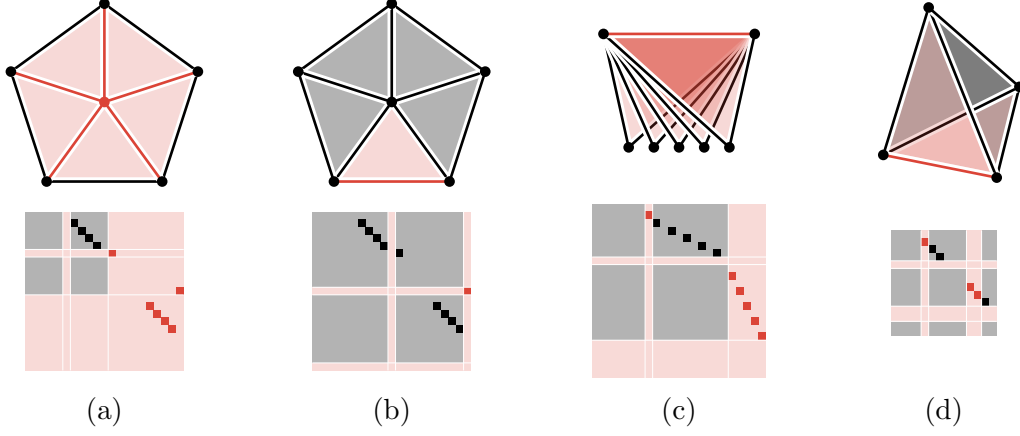


Figure 5: Several examples of how the barcode of a simplicial complex may change when the star of a simplex (highlighted in light red) is removed, as observed in the simplicial complex (top row) and the reduced boundary matrix (bottom row). Finite bars (one in dimension 0 and several in dimension 1) disappear and an infinite bar in dimension 1 appears in (a), a finite bar becomes shorter and another finite bar disappears in (b), 4 infinite bars in dimension 1 appear in (c), and an infinite bar disappears in (d).

that is removed gave birth to a homological class, the dimension of that class must be $\dim(\tau)$, and if it kills a class, it can only kill a class of dimension $\dim(\tau) - 1$.

Remark 4.1. Let \mathcal{F} be a filtration of the factorization $R = DU$ of a simplicial complex containing a simplex τ , and \mathcal{F}' the same filtration with τ removed. Exactly one of the following must occur:

1. The simplex τ is positive (its reduced column in R is a zero column). Then there is an infinite bar in the barcode of \mathcal{F} that disappears in the barcode of \mathcal{F}' .
2. The simplex τ is negative and is not part of the representative cycle of any non-trivial homology class. Then the barcode of \mathcal{F} has a finite bar killed by τ , which becomes an infinite bar in the barcode of \mathcal{F}' .
3. The simplex τ is negative and is part of the representative cycle of some non-trivial homology class. Then the barcode of \mathcal{F} has a finite bar killed by τ , which is longer in the barcode of \mathcal{F}' and is now killed by a coface of τ . In addition, the bar in the barcode of \mathcal{F} corresponding to this coface disappears in the barcode of \mathcal{F}' .

Recall that the representative cycle of a (non-trivial) homology class consists of the simplices associated to the non-empty rows of the column in U at which that class is born.

The cases in Remark 4.1 can be tracked in SiRUP. In case 1, the pivot of the column of the simplex τ is higher (smaller index) than all other pivots, so B from Line 5 is the singleton $\{j\}$, and $k = 0$ for every step in the for-loop of Line 6, and the if-condition in Line 8 is never satisfied. In case 2, the set A of affected simplices from Line 4 is the singleton $\{j\}$, as is B , so the for-loop of Line 6 does not have any steps. In case 3, the set A has at least two elements, the set B has at least one element, and the for-loop of Line 6 has at least one step.

4.3 The necessity of U

The SiRUP algorithm requires keeping track of class representatives in the matrix U , which is more than the minimal amount of information necessary to compute the barcode. This is an advantage as it keeps the representative cycles updated, but it is more memory-consuming than just updating the barcode. One may ask if it is necessary to remember U , in cases in which one knows that the representative cycles are not needed. The answer is no. As Figure 6 demonstrates, it is not possible

to update the barcode after a simplex has been removed by only remembering R , and U contains the information that makes it possible. In Figure 6, the resulting matrix R is the same, but different 1-simplices in different filtrations contributed to zeroing out the same column of e_4 . That is, the effect on the barcode computed by R by removing a simplex is ambiguous, and by checking the matrix U , we can obtain the correct updated barcode.

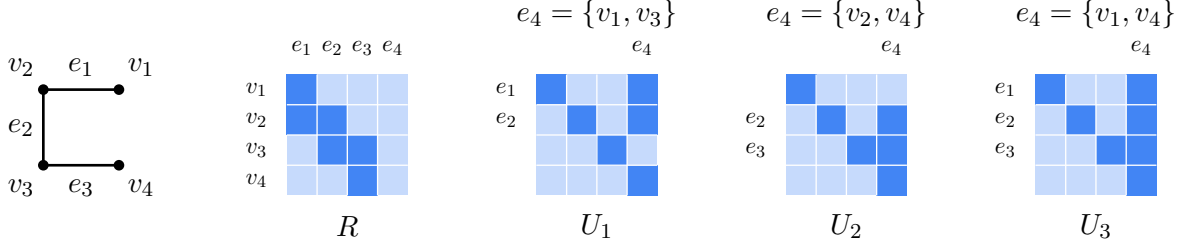


Figure 6: A simplicial complex without the 1-simplex e_4 (left) and three possible matrices U_i for three different choices of e_4 . For D_i the appropriate boundary matrix in each case, all three choices satisfy $\begin{bmatrix} 0 & R \\ 0 & 0 \end{bmatrix} = D_i \begin{bmatrix} I & 0 \\ 0 & U_i \end{bmatrix}$.

4.4 Comparison with other methods

4.4.1 Removal as a dynamic zigzag

Removing a simplex from a filtration can also be realized by expanding the filtration by adding backward maps at the end, thus turning it into a zigzag, where each backward map removes one simplex. Dey and Hou [DH22b; DH24; DH22a] develop an efficient method (called FASTZIGZAG) for computing the persistent homology of zigzag filtrations, defined for a larger class of changes than just simplex removal. Their method is very efficient compared to other zigzag computations, but, unsurprisingly since it is constructed for a more general setting, it is less efficient in practice (even if not asymptotically) than SiRUP for removing simplices. Indeed, as detailed in Example 4.2, for each simplex that needs to be removed, FASTZIGZAG performs $N(2N - 1)$ operations. On the other hand, SiRUP needs at most N^2 operations in general, and 0 in the described example.

Example 4.2. Consider a simplicial complex K on N vertices connected by $N - 1$ edges, arranged as a line graph. Dey–Hou requires simplex-wise filtrations which start and end at \emptyset , but for brevity we consider the truncation of only forward arrows. The omitted right side in Equation (6) is the mirror image of the left side (that is, backward arrows in reverse order of how the simplices were introduced). An example filtration for $N = 4$ is given by

$$\begin{array}{ccccccccccc}
 & & & & & v_4 & & & & & & \\
 & & & & & \bullet & & \bullet & & \bullet & & \bullet \\
 & & & & v_3 & \bullet & & \bullet & & \bullet & & \bullet \\
 & & & v_2 & \bullet & & \bullet & & \bullet & & \bullet & \\
 & & v_1 & \bullet & & & & & & & & \\
 \emptyset & \xrightarrow{v_1} & K_1 & \xrightarrow{v_2} & K_2 & \xrightarrow{v_3} & K_3 & \xrightarrow{v_4} & K_4 & \xrightarrow{e_1} & K_5 & \xrightarrow{e_2} & K_6 & \xrightarrow{e_3} & K_7 & \xleftarrow{e_3} & \dots
 \end{array}
 \tag{6}$$

Removing the edge e_1 is a backwards map $\xleftarrow{e_1}$. This map already appears in the truncated end of Equation (6), and as e_1 is maximal in K , we can move it via backward and outward switches to immediately after the addition of e_1 . This is done so that when computing the barcode, ignoring all bars with endpoints at the introduction or removal step of e_1 will produce the barcode as if e_1 never existed. The associated filtration $\hat{\mathcal{E}}$ required by Dey–Hou of only forward arrows is constructed by replacing a backwards arrow $\xleftarrow{\sigma}$ with a forwards arrow $\xrightarrow{\hat{\sigma}}$ of the cone of the same simplex, coned at the common cone point ω (which has been added before any other simplex), in reverse order of

all the backward arrows. Note that the backwards arrow $\xleftarrow{e_1}$ must be moved again to, to have an “up-down” filtrations. Beginning at the step at which all the simplices of K have been added, this new filtration of a simplicial complex \hat{K} ends in

$$\begin{array}{ccccccccccccccc} \dots & \xrightarrow{e_3} & \hat{K}_7 & \xrightarrow{\hat{v}_1} & \hat{K}_8 & \xrightarrow{\hat{v}_2} & \hat{K}_9 & \xrightarrow{\hat{v}_3} & \hat{K}_{10} & \xrightarrow{\hat{v}_4} & \hat{K}_{11} & \xrightarrow{\hat{e}_1} & \hat{K}_{12} & \xrightarrow{\hat{e}_2} & \hat{K}_{13} & \xrightarrow{\hat{e}_3} & \hat{K}_{14}. \end{array} \quad (7)$$

At this step the filtration of only forward arrows may be reduced directly. The filtrations of the simplicial complexes K, \hat{K} have reduced factorizations $R = DU$ and $\hat{R} = \hat{D}\hat{U}$, respectively, where

$$D = \begin{array}{c} e_1 \\ \begin{array}{|c|c|c|c|c|} \hline \text{blue} & \text{blue} & \text{blue} & \text{blue} & \text{blue} \\ \hline \text{blue} & \text{blue} & \text{blue} & \text{blue} & \text{blue} \\ \hline \text{blue} & \text{blue} & \text{blue} & \text{blue} & \text{blue} \\ \hline \text{blue} & \text{blue} & \text{blue} & \text{blue} & \text{blue} \\ \hline \text{blue} & \text{blue} & \text{blue} & \text{blue} & \text{blue} \\ \hline \end{array} \end{array}, \quad U = \begin{array}{c} \begin{array}{|c|c|c|c|c|} \hline \text{blue} & \text{blue} & \text{blue} & \text{blue} & \text{blue} \\ \hline \text{blue} & \text{blue} & \text{blue} & \text{blue} & \text{blue} \\ \hline \text{blue} & \text{blue} & \text{blue} & \text{blue} & \text{blue} \\ \hline \text{blue} & \text{blue} & \text{blue} & \text{blue} & \text{blue} \\ \hline \text{blue} & \text{blue} & \text{blue} & \text{blue} & \text{blue} \\ \hline \end{array} \end{array}, \quad \hat{D} = \begin{array}{c} e_1 \quad \hat{e}_1 \\ \begin{array}{|c|c|c|c|c|c|c|c|} \hline \text{blue} & \text{blue} & \text{blue} & \text{blue} & \text{blue} & \text{blue} & \text{blue} & \text{blue} \\ \hline \text{blue} & \text{blue} & \text{blue} & \text{blue} & \text{blue} & \text{blue} & \text{blue} & \text{blue} \\ \hline \text{blue} & \text{blue} & \text{blue} & \text{blue} & \text{blue} & \text{blue} & \text{blue} & \text{blue} \\ \hline \text{blue} & \text{blue} & \text{blue} & \text{blue} & \text{blue} & \text{blue} & \text{blue} & \text{blue} \\ \hline \text{blue} & \text{blue} & \text{blue} & \text{blue} & \text{blue} & \text{blue} & \text{blue} & \text{blue} \\ \hline \text{blue} & \text{blue} & \text{blue} & \text{blue} & \text{blue} & \text{blue} & \text{blue} & \text{blue} \\ \hline \text{blue} & \text{blue} & \text{blue} & \text{blue} & \text{blue} & \text{blue} & \text{blue} & \text{blue} \\ \hline \text{blue} & \text{blue} & \text{blue} & \text{blue} & \text{blue} & \text{blue} & \text{blue} & \text{blue} \\ \hline \end{array} \end{array}, \quad \hat{U} = \begin{array}{c} \begin{array}{|c|c|c|c|c|c|c|c|} \hline \text{blue} & \text{blue} & \text{blue} & \text{blue} & \text{blue} & \text{blue} & \text{blue} & \text{blue} \\ \hline \text{blue} & \text{blue} & \text{blue} & \text{blue} & \text{blue} & \text{blue} & \text{blue} & \text{blue} \\ \hline \text{blue} & \text{blue} & \text{blue} & \text{blue} & \text{blue} & \text{blue} & \text{blue} & \text{blue} \\ \hline \text{blue} & \text{blue} & \text{blue} & \text{blue} & \text{blue} & \text{blue} & \text{blue} & \text{blue} \\ \hline \text{blue} & \text{blue} & \text{blue} & \text{blue} & \text{blue} & \text{blue} & \text{blue} & \text{blue} \\ \hline \text{blue} & \text{blue} & \text{blue} & \text{blue} & \text{blue} & \text{blue} & \text{blue} & \text{blue} \\ \hline \text{blue} & \text{blue} & \text{blue} & \text{blue} & \text{blue} & \text{blue} & \text{blue} & \text{blue} \\ \hline \text{blue} & \text{blue} & \text{blue} & \text{blue} & \text{blue} & \text{blue} & \text{blue} & \text{blue} \\ \hline \end{array} \end{array}.$$

SiRUP requires 0 column additions to remove e_1 from the decomposition $R = DU$, as the column of e_1 is not added to any other column, as evidenced by U . Computing \hat{R} by the standard barcode algorithm requires $N(2N - 1) - 1$ more column additions than computing R , as evidenced by \hat{U} .

4.4.2 Removal as a sequence of vine swaps

The method of [CEM06] is adapted by [LN24] to perform a sequence of transpositions in the order of the simplices, moving a simplex that needs to be removed to the end of the filtration and then dropping it. Compared with this approach, SiRUP does not require the operations matrix U to be upper triangular, but we do require updates of U to encode the correct representative cycles. Contrary to what happens with the zigzags case in the previous section, swapping the vines will keep track of the representative cycles. However, it is not as efficient as SiRUP. In general, [CEM06] requires a single column (and row) addition in R (and U) for every simplex with $U[\sigma, i] = 1$, given by Cases 2.1 and 3.1 in [CEM06]. This corresponds to every element (excluding σ) in the list A in SiRUP, and similarly a single addition (of not necessarily the same summands) in each of R and U are performed in each step of the for-loop in Line 6 of SiRUP. Therefore, for every column addition performed by SiRUP, swapping vines has at least one column operation, and thus cannot be more efficient. Moreover, there is at most one more column and row addition required by [CEM06] for each swap, for when pivots change (Cases 1.1.2, 2.1.2 in [CEM06]) as a result of the swap. In contrast, no more additions are ever required by SiRUP. Hence the method of [CEM06; LN24] takes at least as many steps as SiRUP, to produce the same updated persistence pairs, with a potentially different $R = DU$ factorization.

In practice, swapping vineyards may incur $O(n)$ more operations than SiRUP. For a practical example, consider the filtration in Figure 5 (c), with $N = 5$ simplices in dimension 2. To remove the star of the 1-simplex, SiRUP performs one column addition in R and N column additions in U , as all of the columns to which the 1-simplex was added are zero. Conversely, [CEM06] would perform $N + 1$ column additions in both R and U , as well as $2N$ column transpositions in R, U for the same task.

To further illustrate the difference, we can use the filtration described in Example 4.2. We can use a sequence of swaps to move e_1 and \hat{e}_1 to the end of the filtration $\hat{\mathcal{E}}$. This would require $2(N - 1)$ column additions, as the algorithm SBA adds the column of e_1 to each of the columns of the coned vertices exactly once (except the first one), corresponding to Case 3.1 in [CEM06] and producing two column operations each.

5 Implementation and testing

We have implemented SiRUP in a publicly available repository PHAT-SiRUP[GL24], and have performed tests to demonstrate its feasibility (Section 5.2). We performed several experiments on a diverse set of inputs, recording both the time necessary to complete the experiments and the number of operations needed, with code to generate and execute the tests described also publicly available on Zenodo [GL25]. Our main results, presented visually in Figure 7 and in more detail in Table 4, demonstrate that updating representative cycles and the barcode with SiRUP is always faster and takes less matrix operations than doing the same with PHAT-op (PHAT software that also keeps track of the operations matrix). Even when comparing with a task that does less, only computing the barcode from scratch with PHAT, SiRUP is still almost always faster on tests that remove up to 200 simplices.

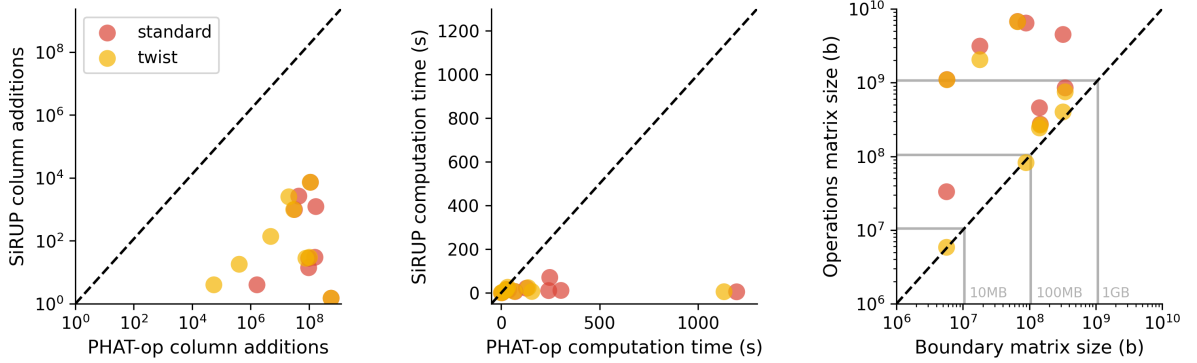


Figure 7: A visual overview of our main testing results. The plots are colored semi-transparently to distinguish the cases when there is little difference between the `--standard` and `--twist` methods. File sizes of boundary and operations matrices are also compared (bottom right), highlighting the tradeoff in time for space for SiRUP. The full details of the left and center plots are given in Table 4. Raw data for all three plots is given in the related dataset [GL25].

5.1 Implementation

The implementation of SiRUP, named PHAT-SiRUP, is built on top of the methods of the Persistent Homology Algorithm Toolbox (PHAT) [Bau+17], a collection of C++ headers to compute persistence pairs of a simplicial complex filtration. This software was chosen because we wanted to compare just the reduction routine, which is precisely the focus of PHAT. Nevertheless, any software that takes in a list of simplices and computes persistence pairs by way of operations on the boundary matrix is amenable to an implementation of SiRUP. While the current implementation of PHAT-SiRUP is already more efficient in most cases than recomputing from scratch, it is still a proof-of-concept: the look-up operations in PHAT-SiRUP have potential to be considerably optimized with a more suitable data structure. Moreover, a proper implementation should include not just removal but integrate the swaps and additions of simplices from the literature, which goes beyond the scope of the current paper. Here, the focus has been to accurately reflect SiRUP (Algorithm 2) and demonstrate its role as a theoretical improvement over the current state-of-the-art.

5.2 Testing

Our experiments have been run on a computer with an Intel Core i7-8650U CPU with eight 1.9GHz cores and 15.4GiB of RAM, running Ubuntu 22.04 LTS, with gcc version 11.4.0. The implementation is not parallelized. Random selection of the simplices was done with `std::random_device` seeding the pseudo-random generator `std::mt19337`. Timing of the individual parts of the code was done

with `omp_get_wtime`, and of the full execution by reading the `SECONDS` variable within the `bash` command interpreter of Linux.

Inputs. The datasets are either taken from [Ott+17; Ega+25; ST18; Kla] or generated randomly with [Har+20]. They are chosen to be as large as possible, while still being computationally manageable, and to demonstrate the strengths and weaknesses of SiRUP. A full overview of the datasets and associated topological constructions is given in Tables 2 and 3.

Dataset	0-dim	1-dim	2-dim	3-dim	4-dim	Source
<code>vr_dsphere</code>	3 000	65 052	400 187	1 224 795	2 353 767	[ST18; Lüt+20]
<code>vr_torus</code>	1 000	21 988	214 105	1 415 261	7 288 105	[ST18; Lüt+20]
<code>vr_senate</code>	103	5 253	176 851	4 421 275	0	[Ott+17; Lüt+20]
<code>er_clique</code>	100	4 463	118 583	2 111 092	0	[Har+20; Lüt+20]
<code>er_shuffled</code>	100	3 005	36 126	194 908	0	[Har+20; Lüt+20]
<code>alpha_cube</code>	10 000	76 644	133 170	66 525	0	[ST18; Bau+24]
<code>alpha_swissroll</code>	100 000	1 043 027	1 829 784	886 756	0	[ST18; Bau+24]
<code>cc_tooth</code>	1 558 802	4 635 007	4 593 966	1 517 760	0	[Kla; Bau+24]
<code>bio_bbmcl6</code>	3 174	180 032	529 470	157 900	0	[Ega+25; Lüt+20]

Table 2: Descriptive overview of input datasets, with the number of simplices by dimension, and sources for sampling and construction indicated. The filtrations on each dataset that result in the complexes with the given numbers of simplices are described in Table 3.

We used five different types of filtrations (**Vietoris–Rips**, **alpha**, **random**, **lowerstar**, and **biological**) on two different types of complexes (**simplicial** and **cubical**), chosen for their common use in practice. We will not define these filtrations here, but the unfamiliar reader may look the definitions up in [Ott+17] (the first four) and [Mar+15] (the latter). The **clique** filtration was used together with the random filtration, by first randomly selecting the order of edges, then including simplices for all resulting cliques, also in a random order. All complexes were simplicial complexes, except for `cc_tooth`, which was a cubical complex defined by a three-dimensional scan of a tooth. Random sampling for simplicial complexes based on Erdős–Rényi graphs is done with NumPy [Har+20]. Identifying higher dimensional simplices for Vietoris–Rips and Erdős–Rényi constructions is done with the FLAGSER-COUNT [Smi24] variant of FLAGSER [Lüt+20]. Full descriptions of the filtrations are given in Table 3.

Dataset	Filtration	Description
<code>vr_dsphere</code> <code>vr_torus</code> <code>vr_senate</code>	Vietoris–Rips	Random samples over a unit 4-sphere in \mathbf{R}^6 , random samples over a 2-torus with major radius 2 and minor radius 1 in \mathbf{R}^4 , and a legislator voting dataset (distances among 103 points) from [Ott+17]. Both random samples have normally distributed noise at standard deviation 0.2. Only edges less than 0.6 are considered for <code>vr_dsphere</code> , and less than 1 for <code>vr_torus</code> . All edges are considered for <code>vr_senate</code> .
<code>er_clique</code> <code>er_shuffled</code>	random, clique	Random values in $[0, 1]$ assigned to $\binom{100}{2}$ edges, included from highest to lowest “probability,” with higher dimensional simplices defined by the clique complex. For <code>er_clique</code> , a $(d > 1)$ -simplex is ordered immediately after all its faces. For <code>er_shuffled</code> , the order of every $(d > 1)$ -simplex is included in a random order after all its faces have been included. Probability at least 0.1 considered for <code>er_clique</code> and at least 0.5 for <code>er_shuffled</code> .
<code>alpha_cube</code> <code>alpha_swissroll</code>	alpha	Random samples of 10 000 and 100 000 points over a cube and swiss, respectively, generated with [ST18].
<code>cc_tooth</code>	lowerstar, clique	A 3D image of a tooth from [Kla], represented as a $104 \times 91 \times 161$ array of values in $[0, 255]$. This defines a filtration of a cubical complex in 3 dimensions.
<code>bio_bbmcl6</code>	biological, clique	Biologically motivated reconstruction of a rat’s neocortex [Mar+15], with neurons as vertices, synapses as edges, and their clique complex defining higher dimensional simplices. Restricted to the undirected excitatory subcircuit of bipolar pyramidal cells in Layer 6 ($\approx 10\%$ of all the neurons).

Table 3: Details of filtrations on input datasets.

Updates. For each dataset, a fixed number of simplices was selected to be removed in one of the dimensions of the complex. The union of the stars of those simplices was computed, producing an update file with the indices of all the simplices to be removed, and an updated boundary matrix

without those simplices. The number of simplices, by dimension and in total, is reported in the second column of Table 4.

Dataset	Simplices removed	Number of column additions						Computation time in seconds					
		SiRUP		PHAT-op (M)		PHAT (M)		SiRUP		PHAT-op		PHAT	
		std	twi	std	twi	std	twi	std	twi	std	twi	std	twi
vr_dsphere	183 (0,1,15,59,108)	2640	2508	89.8	42.3	44.9	20.5	13.7	11.9	37.5	21.8	17.6	10.2
vr_torus	5 (0,0,0,0,5)	28	28	195.8	158.9	97.9	78.7	6.0	6.6	70.4	66.7	36.3	33.2
vr_senate	20 (0,0,0,20)	990	990	63.6	60.4	31.8	30.1	15.3	15.4	26.9	26.0	12.5	12.4
er_clique	3 (0,0,0,3)	0	0	1150.0	1141.6	576.8	570.8	4.7	5.1	1196.3	1132.2	429.9	394.8
er_shuffled	25 (0,0,1,24)	7268	7278	225.1	222.7	112.6	111.3	21.1	23.6	128.4	136.7	55.5	61.2
alpha_cube	5 (0,0,0,5)	4	4	3.3	0.3	1.7	0.1	0.2	0.1	3.8	0.6	1.3	0.2
alpha_swissroll	9 (0,1,4,4)	14	18	195.3	2.7	97.6	0.4	10.3	3.0	241.3	7.1	68.2	2.2
cc_tooth	27 (1,6,12,8)	1228	138	344.9	15.9	172.4	4.9	70.5	25.5	246.7	32.9	93.5	12.3
bio_bbmcl6	8 (0,1,6,1)	30	30	320.9	207.9	160.5	103.8	11.0	6.3	303.7	155.7	77.9	42.7

Table 4: Experiments comparison between SiRUP, PHAT-op, and PHAT, indicating the number of simplices removed (in parentheses in increasing dimension) from each filtration. Number of column additions (in millions “M” for PHAT-op and PHAT) and computations time (in seconds, excluding file reading and writing) are given for the standard reduction method and with the twist optimization [CK11], abbreviated **std** and **twi**, respectively. The best results are indicated in bold. A visual representation of the testing process and results is given in Figure 8.

Testing pipeline. The performance of SiRUP was tested against PHAT-op, the name we give to the PHAT software modified to keep track of the operations matrix U in the decomposition $R = DU$. This is done so that both programs perform the same task, and the work done is comparable. The performance of PHAT was also analyzed on the same task, but without requiring representative cycles, to demonstrate that even if only the barcode is requested, SiRUP still executes less column additions in a comparable time. The comparisons among these three programs on the described inputs is given in Table 4, and a visual overview of the pipeline and key results is given in Figure 8. Counting the number of column operations was tested separately from timing the computation, as the recording and output the count is itself a time-intensive process. Read and write times of files were recorded, but are not considered here. The full code and execution steps are provided in a public repository [GL25].

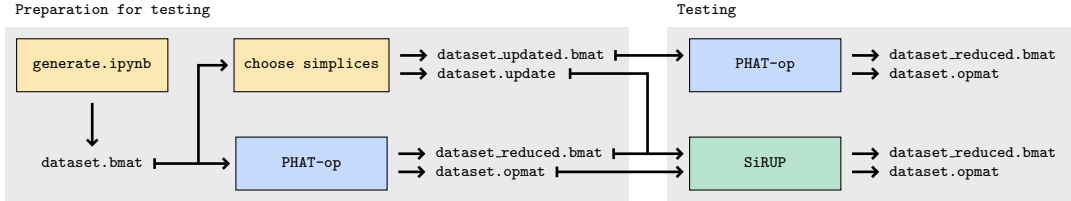


Figure 8: Steps and outputs of full testing environment. The values reported in Table 4 are from execution of SiRUP and PHAT-op in the “Testing” stage (right).

5.2.1 Counting column additions

The strength of SiRUP is from the vastly smaller number of column additions that need to be done to update the representative cycles and barcode, as shown in Table 4. Note that in the case of **er_clique**, there are no column additions that are done by SiRUP, indicating that the simplices to be removed were not added to other simplices in the reduction, and only their columns need to be deleted and the complex reindexed. In the same situation PHAT executes more than 500 million column additions to arrive at a result that was already computed once before.

5.2.2 Timing algorithm execution

As seen in Table 4, in almost all cases SiRUP is faster than recomputing from scratch using PHAT, and is always considerably faster than using PHAT-op and computing the representative cycles. The difference is not only related to the number of simplices removed, as for `vr_dsphere` considering the impact of ≈ 180 simplices is still faster than computing from scratch. Recall that only the computation time is recorded in Table 4, not the file reading in and writing out times. As demonstrated in Figure 8 (bottom right), the files sizes may be quite large and may add an additional time cost. The data structure for operations matrices is the same as the one for boundary matrices in PHAT. However, in the case that the matrices are loaded in memory and are repeatedly being updated, the read/write times are not relevant. These experiments suggest that SiRUP is more efficient in practice under small changes, with room for improvement in memory management and appropriate data structures.

6 Discussion and future work

We presented an efficient method to update the barcode of a filtration and its representative cycles when simplices are removed. We proved that our method is asymptotically better than recomputing the barcode from scratch, minimal in the amount of column additions, and we provided constructions on which our method performs asymptotically better than other methods in the literature which can be adapted to produce our output [DH22b; CEM06], showing that the other way around is not possible. Finally, we validated our theoretical results with experiments showing that the computational time of our algorithm is often considerably better than recomputing from scratch, especially with a small number of changes.

A key improvement necessary for our implementation is decreasing the reading and writing time, as it is now a bottleneck for practical uses, and optimize the look-up of columns in SiRUP, since the number of column additions is already reduced to the minimum. In particular, a more efficient method to find all columns with $V[j, i] \neq 0$ for a given j would provide a significant speed up, as currently the algorithm iterates through every column in a given dimension for each simplex to be removed. Note that SiRUP can also be modified to include several variants of the SBA [Bau+24]. Finally, we plan to implement a fully dynamic barcode pipeline, merging the existing algorithms for all three type of changes in the filtration (simplex additions, simplex swaps, and simplex removal). A general algorithm and implementation for all changes exists [LN24], but with more than the minimal number of column additions for simplex removal of SiRUP.

Applications of our method, discussed in Section 1.1, may require to remove a half or a third of simplices in a given filtration. In the case that the columns of the simplices to be removed interact with each other and not with the columns of the simplices that remain, one could try to skip even more operations than presented here. However, implementing this observation is not straightforward and will require care, as some operations affecting only columns-to-be-removed may compound and impact the columns of simplices that stay. We plan to improve our implementation to take this scenario into account, improving efficiency by considering overall implications of the full set of simplices to be removed.

Acknowledgements. B.G. was partially supported by the Austrian Science Fund (FWF) P 33765-N. J.L. was partially supported by EPSRC grant EP/P025072/1 “Topological Analysis of Neural Systems”, and by the Latvian Council of Science (LZP) 1.1.1.9 Research application No 1.1.1.9/LZP/1/24/125 of the Activity “Post-doctoral Research” “Efficient topological signatures for representation learning in medical imaging”. J.L. thanks the Austrian Science Fund (FWF) P 33765-N and Prof. Michael Kerber at Graz University of Technology for hosting him during a research visit on this project. The authors are thankful to Michael Kerber, David Millman, and Felix Ye for useful preliminary discussions, and to anonymous reviewers for constructive feedback.

References

- [AP23] Manu Aggarwal and Vipul Periwal. “Tight basis cycle representatives for persistent homology of large biological data sets”. In: *PLoS Comput Biol* 19.5 (2023), e1010341.
- [ATV14] Henry Adams, Andrew Tausz, and Mikael Vejdemo-Johansson. “JavaPlex: A research software package for persistent (co)homology”. In: *Mathematical Software – ICMS 2014*. Vol. 8592. Lecture Notes in Computer Science: Springer Berlin Heidelberg, 2014, pp. 129–136.
- [Bau+17] Ulrich Bauer, Michael Kerber, Jan Reininghaus, and Hubert Wagner. “Phat–persistent homology algorithms toolbox”. In: *Journal of Symbolic Computation* 78 (2017), pp. 76–90.
- [Bau+24] Ulrich Bauer, Talha Bin Masood, Barbara Giunti, Guillaume Houry, Michael Kerber, and Abhishek Rathod. “Keeping it sparse: Computing Persistent Homology revisited”. In: *Computing in Geometry and Topology* 3.1 (2024), 6:1–6:26.
- [Bau21] Ulrich Bauer. “Ripser: efficient computation of Vietoris–Rips persistence barcodes”. In: *Journal of Applied and Computational Topology* 5.3 (2021), pp. 1–33.
- [BKR14] Ulrich Bauer, Michael Kerber, and Jan Reininghaus. “Clear and Compress: Computing Persistent Homology in Chunks”. In: *Topological Methods in Data Analysis and Visualization III, Theory, Algorithms, and Applications*. Springer, 2014, pp. 103–117.
- [CEF13] Andrea Cerri, Marc Ethier, and Patrizio Frosini. “A Study of Monodromy in the Computation of Multidimensional Persistence”. In: *Discrete Geometry for Computer Imagery*. Springer Berlin Heidelberg, 2013, pp. 192–202.
- [CEM06] David Cohen-Steiner, Herbert Edelsbrunner, and Dmitriy Morozov. “Vines and Vineyards by Updating Persistence in Linear Time”. In: *Proceedings of the Twenty-Second Annual Symposium on Computational Geometry*. New York, NY, USA: Association for Computing Machinery, 2006, pp. 119–126.
- [CK11] Chao Chen and Michael Kerber. “Persistent homology computation with a twist”. In: *Proceedings 27th European Workshop on Computational Geometry*. 2011.
- [Col+22] Gloria Colombo, Ryan John A. Cubero, Lida Kanari, Alessandro Venturino, Rouven Schulz, Martina Scolamiero, Jens Agerberg, Hansruedi Mathys, Li-Huei Tsai, Wojciech Chachólski, Kathryn Hess, and Sandra Siegert. “A tool for mapping microglial morphology, morphOMICs, reveals brain-region and sex-dependent phenotypes”. In: *Nature Neuroscience* 25.10 (2022), pp. 1379–1393.
- [Con+22] Pedro Conceição, Dejan Govc, Jānis Lazovskis, Ran Levi, Henri Riihimäki, and Jason P. Smith. “An application of neighbourhoods in digraphs to the classification of binary dynamics”. In: *Network Neuroscience* 6.2 (2022), pp. 528–551.
- [DH22a] Tamal K. Dey and Tao Hou. “Fast Computation of Zigzag Persistence”. In: *30th Annual European Symposium on Algorithms (ESA 2022)*. Vol. 244. Leibniz International Proceedings in Informatics (LIPIcs). Schloss Dagstuhl – Leibniz-Zentrum für Informatik, 2022, 43:1–43:15.
- [DH22b] Tamal K. Dey and Tao Hou. *Updating Barcodes and Representatives for Zigzag Persistence*. Preprint available at arXiv:2112.02352. 2022.
- [DH24] Tamal K. Dey and Tao Hou. “Computing Zigzag Vineyard Efficiently Including Expansions and Contractions”. In: *40th International Symposium on Computational Geometry (SoCG 2024)*. Leibniz International Proceedings in Informatics (LIPIcs). Schloss Dagstuhl – Leibniz-Zentrum für Informatik, 2024, 49:1–49:15.
- [DW22] Tamal Krishna Dey and Yusu Wang. *Computational Topology for Data Analysis*. Cambridge University Press, 2022.
- [Ede+04] Herbert Edelsbrunner, John Harer, Ajith Mascarenhas, and Valerio Pascucci. “Time-varying reeb graphs for continuous space-time data”. In: *Proceedings of the Twentieth Annual Symposium on Computational Geometry*. SCG ’04. Association for Computing Machinery, 2004, pp. 366–372. ISBN: 1581138857.
- [Ega+25] Daniela Egas Santander, Christoph Pokorný, András Ecker, Jānis Lazovskis and Matteo Santoro, Jason P. Smith, Kathryn Hess, Ran Levi, and Michael W. Reimann. “Heterogeneous and higher-order cortical connectivity undergirds efficient, robust, and reliable neural codes”. In: *iScience* 28.1 (2025), p. 111585.

- [EH10] Herbert Edelsbrunner and John L. Harer. *Computational topology: An introduction*. Vol. 69. American Mathematical Society, Providence, RI, 2010, pp. xii+241.
- [ELZ00] Herbert Edelsbrunner, David Letscher, and Afra Zomorodian. “Topological persistence and simplification”. In: *Proceedings 41st annual symposium on foundations of computer science*. IEEE. 2000, pp. 454–463.
- [Giu21] Barbara Giunti. “Notes on pivot pairings”. In: *Proceedings of the 37th European Workshop on Computational Geometry*. 2021, 11:1–11:6.
- [GL24] Barbara Giunti and Jānis Lazovskis. PHAT-VINEYARDS. <https://bitbucket.org/jlazovskis/phant-vineyards/src/master/>. (2024).
- [GL25] Barbara Giunti and Jānis Lazovskis. *Dataset for “Pruning vineyards: updating barcodes and representative cycles by removing simplices”*. 2025. DOI: 10.5281/zenodo.15481043.
- [GLR22] Barbara Giunti, Jānis Lazovskis, and Bastian Rieck. *DONUT: Database of Original & Non-Theoretical Uses of Topology*. <https://donut.topology.rocks>. 2022.
- [Har+20] Charles R. Harris, K. Jarrod Millman, Stéfan J. van der Walt, Ralf Gommers, Pauli Virtanen, David Cournapeau, Eric Wieser, Julian Taylor, Sebastian Berg, Nathaniel J. Smith, Robert Kern, Matti Picus, Stephan Hoyer, Marten H. van Kerkwijk, Matthew Brett, Allan Haldane, Jaime Fernández del Río, Mark Wiebe, Pearu Peterson, Pierre Gérard-Marchant, Kevin Sheppard, Tyler Reddy, Warren Weckesser, Hameer Abbasi, Christoph Gohlke, and Travis E. Oliphant. “Array programming with NumPy”. In: *Nature* 585.7825 (2020), pp. 357–362.
- [HG16] Gregory Henselman and Robert Ghrist. *Matroid filtrations and computational persistent homology*. Preprint available at arXiv:1606.00199. 2016.
- [Hic23] Abigail Hickok. *Persistence Diagram Bundles: A Multidimensional Generalization of Vineyards*. Preprint available at arXiv:2210.05124. 2023.
- [Kla] Pavol Klacansky. *Open Scientific Visualization Datasets*. <https://klacansky.com/open-scivis-datasets/>.
- [KMS20] Woojin Kim, Facundo Mémoli, and Zane Smith. “Analysis of Dynamic Graphs and Dynamic Metric Spaces via Zigzag Persistence”. In: *Topological Data Analysis*. Springer International Publishing, 2020, pp. 371–389.
- [Li+21] Lu Li, Connor Thompson, Gregory Henselman-Petrusek, Chad Giusti, and Lori Ziegelmeier. “Minimal Cycle Representatives in Persistent Homology Using Linear Programming: An Empirical Study With User’s Guide”. In: *Front Artif Intell* 4 (2021), p. 681117.
- [LN24] Yuan Luo and Bradley J. Nelson. “Accelerating iterated persistent homology computations with warm starts”. In: *Computational Geometry* 120 (2024), p. 102089.
- [Lüt+20] Daniel Lütgehetmann, Dejan Govc, Jason P. Smith, and Ran Levi. “Computing Persistent Homology of Directed Flag Complexes”. In: *Algorithms* 13.1 (2020).
- [Mar+15] Henry Markram, Eilif Muller, Srikanth Ramaswamy, Michael W Reimann, Marwan Abdellah, Carlos Aguado Sanchez, Anastasia Ailamaki, Lidia Alonso-Nanclares, Nicolas Antille, Selim Arsever, Guy Antoine Atenekeng Kahou, Thomas K Berger, Ahmet Bilgili, Nenad Buncic, Athanassia Chalimourda, Giuseppe Chindemi, Jean-Denis Courcol, Fabien Delalondre, Vincent Delattre, Shaul Druckmann, Raphael Dumusc, James Dynes, Stefan Eilemann, Eyal Gal, Michael Emiel Gevaert, Jean-Pierre Ghobril, Albert Gidon, Joe W Graham, Anirudh Gupta, Valentin Haenel, Etay Hay, Thomas Heinis, Juan B Hernando, Michael Hines, Lida Kanari, Daniel Keller, John Kenyon, Georges Khazen, Yihwa Kim, James G King, Zoltan Kisvarday, Pramod Kumbhar, Sébastien Lasserre, Jean-Vincent Le Bé, Bruno R C Magalhães, Angel Merchán-Pérez, Julie Meystre, Benjamin Roy Morrice, Jeffrey Muller, Alberto Muñoz-Céspedes, Shruti Muralidhar, Keerthan Muthurasa, Daniel Nachbaur, Taylor H Newton, Max Nolte, Aleksandr Ovcharenko, Juan Palacios, Luis Pastor, Rodrigo Perin, Rajnish Ranjan, Imad Riachi, José-Rodrigo Rodríguez, Juan Luis Riquelme, Christian Rössert, Konstantinos Sfyraakis, Ying Shi, Julian C Shillcock, Gilad Silberberg, Ricardo Silva, Farhan Tauheed, Martin Telefont, Maria Toledo-Rodriguez, Thomas Tränkle, Werner Van Geit, Jafet Villafranca Díaz, Richard Walker, Yun Wang, Stefano M Zaninetta, Javier DeFelipe, Sean L Hill, Idan Segev, and Felix Schürmann. “Reconstruction and Simulation of Neocortical Microcircuitry”. In: *Cell* 163.2 (2015), pp. 456–492.

- [Moo+20] Michael Moor, Max Horn, Bastian Rieck, and Karsten Borgwardt. “Topological Autoencoders”. In: *Proceedings of the 37th International Conference on Machine Learning*. Ed. by Hal Daumé III and Aarti Singh. Vol. 119. Proceedings of Machine Learning Research. PMLR, 2020, pp. 7045–7054.
- [Mor10] Dmitriy Morozov. *Dionysus Library for Computing Persistent Homology*. Retrieved from mrzv.org/software/dionysus. 2010.
- [Oes+17] Patrick Oesterling, Christian Heine, Gunther H. Weber, Dmitriy Morozov, and Gerik Scheuermann. “Computing and Visualizing Time-Varying Merge Trees for High-Dimensional Data”. In: *Topological Methods in Data Analysis and Visualization IV*. Ed. by Hamish Carr, Christoph Garth, and Tino Weinkauff. Springer International Publishing, 2017.
- [Ott+17] Nina Otter, Mason A Porter, Ulrike Tillmann, Peter Grindrod, and Heather A Harrington. “A roadmap for the computation of persistent homology”. In: *EPJ Data Science* 6 (2017), pp. 1–38.
- [Oud15] Steve Y. Oudot. *Persistence theory: from quiver representations to data analysis*. Vol. 209. Mathematical Surveys and Monographs. American Mathematical Society, Providence, RI, 2015.
- [Pér+21] Julián Burella Pérez, Sydney Hauke, Umberto Lupo, Matteo Caorsi, and Alberto Dassatti. *Giotto-ph: A Python Library for High-Performance Computation of Persistent Homology of Vietoris–Rips Filtrations*. Preprint available at arXiv:2107.05412. 2021.
- [PH15] Jose A. Perea and John Harer. “Sliding Windows and Persistence: An Application of Topological Methods to Signal Analysis”. In: *Foundations of Computational Mathematics* 15.3 (2015), pp. 799–838.
- [Rei+17] Michael W. Reimann, Max Nolte, Martina Scolamiero, Katharine Turner, Rodrigo Perin, Giuseppe Chindemi, Paweł Dłotko, Ran Levi, Kathryn Hess, and Henry Markram. “Cliques of Neurons Bound into Cavities Provide a Missing Link between Structure and Function”. In: *Frontiers in Computational Neuroscience* 11 (2017). ISSN: 1662-5188.
- [Smi24] Jason P. Smith. FLAGSER-COUNT. <https://github.com/JasonPSmith/flagser-count>. 2024.
- [ST18] Nathaniel Saul and Chris Tralie. *TaDAset - a Scikit-TDA project*. <https://github.com/scikit-tda/tadatasets>. 2018. DOI: 10.5281/zenodo.2533369.
- [The15] The GUDHI Project. *GUDHI User and Reference Manual*. GUDHI Editorial Board, 2015. URL: <http://gudhi.gforge.inria.fr/doc/latest/>.